



A novel catheter interaction simulating method for virtual reality interventional training systems

Peng Shi^{1,3} · Shuxiang Guo^{2,3} · Xiaoliang Jin^{3,4} · Hideyuki Hirata³ · Takashi Tamiya⁵ · Masahiko Kawanishi⁵

Received: 10 March 2022 / Accepted: 9 December 2022
© International Federation for Medical and Biological Engineering 2022

Abstract

Endovascular robotic systems have been applied in robot-assisted interventional surgery to improve surgical safety and reduce radiation to surgeons. However, this surgery requires surgeons to be highly skilled at operating vascular interventional surgical robot. Virtual reality (VR) interventional training systems for robot-assisted interventional surgical training have many advantages over traditional training methods. For virtual interventional radiology, simulation of the behaviors of surgical tools (here mainly refers to catheter and guidewire) is a challenging work. In this paper, we developed a novel virtual reality interventional training system. This system is an extension of the endovascular robotic system. Because the master side of this system can be used for both the endovascular robotic system and the VR interventional training system, the proposed system improves training and reduces the cost of education. Moreover, we proposed a novel method to solve catheterization modeling during the interventional simulation. Our method discretizes the catheter by the collision points. The catheter between two adjacent collision points is treated as thin torsion-free elastic rods. The deformation of the rod is mainly affected by the force applied at the collision points. Meanwhile, the virtual contact force is determined by the collision points. This simplification makes the model more stable and reduces the computational complexity, and the behavior of the surgical tools can be approximated. Therefore, we realized the catheter interaction simulation and virtual force feedback for the proposed VR interventional training system. The performance of our method is experimentally validated.

Keywords Catheter interaction simulation · VR interventional training system · Endovascular intervention · Catheter and guidewire · Virtual interventional radiology · Surgical simulation and training

✉ Shuxiang Guo
guoshuxiang@bit.edu.cn
Peng Shi
shipeng@haust.edu.cn

¹ School of Medical Technology and Engineering, Henan University of Science and Technology, Luoyang 471023, China

² Key Laboratory of Convergence Medical Engineering System and Healthcare Technology, the Ministry of Industry and Information Technology, Beijing Institute of Technology, No. 5, Zhongguancun South Street, Haidian District, Beijing 100081, China

³ Faculty of Engineering and Design, Kagawa University, 2217-20 Hayashi-Cho, Takamatsu 760-8521, Japan

⁴ State Key Laboratory of Bioelectronics and the Jiangsu Key Laboratory of Remote Measurement and Control, School of Instrument Science and Engineering, Southeast University, Nanjing 210096, China

⁵ Department of Neurological Surgery, Faculty of Medicine, Kagawa University, Takamatsu 761-0793, Japan

1 Introduction

Minimally invasive surgeries (MIS) have become the most common surgical techniques of treating cardiovascular diseases such as the atherosclerosis, thrombus, and aneurisms [1]. However, prolonged exposure to X-ray radiation during surgery has impact on the interventionalists' health [2]. Endovascular robotic systems have been developed to release surgeon from the risks of radiation and heavy radiation-shielded garments [3–5]. This system allows operators to manipulate surgical tools via master side over a long distance. Moreover, endovascular robotic systems have higher operating accuracy and can assist surgeon to perform more sophisticated surgical operation [6–8].

Robot-assisted interventional surgery requires surgeons to be highly skilled at manipulating vascular interventional surgical robot. Compared with traditional MIS, the use of robots for surgery has changed surgeons' surgical habits [9]. Surgeons need to be trained at endovascular robotic

system to adapt to robot-assisted interventional surgery. In addition, traditional interventional training methods, including using live animals, human cadavers, and vascular phantom, have many limitations such as expensive, risky, and limited morphological models [10]. Virtual reality interventional training systems were developed as a means of improving training and reducing the costs of education. Computer-based simulation of catheterization procedures provides a versatile solution and can virtually be reused infinite times on both common and rare cases. Moreover, patient-specific data can be quickly adopted to regenerate the virtual environment, which provides tools for surgeons to plan or rehearse preoperatively to evaluate and optimize the tentative surgical procedure [11]. Although the VR interventional training has many advantages, the interventional simulation is still not realistic enough compared with traditional training methods. For interventional simulation, one of the most challenging works is to faithfully reproduce the behaviors of surgical tools, including the deformation and virtual contact force.

To predict complex behaviors of surgical tools, several approaches have been proposed [12]. Duriez et al. proposed an incremental finite element method (FEM) to simulate the catheter navigation [13]. The vessel geometry puts strict position constraints upon the catheter. Considering the non-linearities arising from large catheter deformation, the incremental FEM method exists a cumulative error on the catheter shape. Li et al. proposed an improved FEM approach based on the principle of minimal total potential energy [14, 15]. Alderliesten et al. modeled the device as linked rigid bodies based on multi-body dynamics. With complex bending energy and material properties incorporated, this method achieved high accuracy along with a heavy computational workload, especially as the number of connected joints increased [16, 17].

Mass-spring catheter models have been proposed as well [18, 19]. These models are very efficient but cannot ensure to preserve the overall catheter length, since this causes these equations to become numerically stiff and hard to compute. Alderliesten et al. designed a method relying on a quasi-static minimum energy principle [20]. The method departs from the observation that dynamic effects can often be ignored as motions take place in a heavily dampened environment and are generally fairly slow. The argument is that the guidewire (and, by extension, the catheter) thus has the time to relax and take on a configuration where the overall energy of the system, consisting of the potential energy due to deformation of the catheter and the surrounding vessel structure, is minimal. This method has been extensively validated on guidewire motion but is here expanded to predict and control catheter motion [21].

In this paper, we develop a novel virtual reality interventional training system. In addition, a novel method is

proposed to simulate the behaviors of surgical tools, including the deformation and virtual contact force. Our method discretizes the catheter by the collision points. For each part between two adjacent collision points, the catheter is treated as a thin torsion-free elastic rod. Therefore, the catheter model is a structure composed of a set of elastic rods with different length. Based on this assumption, a novel numerical model is proposed to simulate the deformation of the catheter. The contributions of this research are as follows:

1. The master side of the developed VR interventional training system can also be used in the endovascular robotic system [1]. This design improves training and reduces the cost of education.
2. The proposed simulation method can simulate both deformation and virtual contact force. The visual and haptic feedback can increase the realism of the interventional simulation.

The remainder of this paper is organized as follows. The overview of the developed VR interventional training system is presented in Section. 2. Section 3 illustrates the proposed catheter behaviors simulation method. In Section. 4, evaluation experiments are presented to verify the performance of the method. Finally, the conclusion is given in Section. 5.

2 Virtual reality interventional training system

In robot-assisted interventional surgery, surgeon relies on visual and haptic feedback to avoid damaging the blood vessel and guide the catheter to the target area. Therefore, we need to realize two functions for the VR interventional training system: visual feedback and haptic feedback. The haptic feedback is used to provide virtual contact force to the operator during the simulation. This can remind surgeons to avoid damaging blood vessel with excessive force. Visual feedback consists of two parts. One is the simulation of the vasculature, and another is simulation of the behaviors of surgical tools (here mainly refers to the catheter and guidewire). Mesh representation of vasculature and multiple devices interaction is fundamental to interventional simulation.

In order to achieve the above functions, our VR interventional training system includes the master side and VR simulator, as shown in Fig. 1.

2.1 Master side

In the context of interventional simulation for robot-assisted interventional surgery, the surgeon manipulates the virtual catheter by operating the master side and senses the haptic force provided by haptic force interface. Therefore, the

master side needs to realize two functions: measuring the motion of operator (provided by measurement device) and providing the haptic force to operator (provided by haptic force interface). The master side of the developed VR interventional training system is shown in Fig. 2a.

2.1.1 Measurement device

To measure the motion (translation and rotation) of the input catheter, a photoelectric-based sensor platform is utilized in measurement device, as shown in Fig. 2b. This photoelectric-based sensor platform contains two mutually perpendicular photoelectric sensors, two encoder rollers, and one transmission ball. The transmission ball contacts with the input catheter. When the surgeon manipulates the input catheter, the transmission ball will rotate. Two photoelectric sensors will divide this action into the linear motion and rotational motion.

2.1.2 Haptic force interface

To provide haptic force feedback, a spring-based force generator is utilized in haptic force interface, as shown in Fig. 2c. The main function for the force generator is to generate a smoothly changing force. This force generator includes a coil spring, an L-connector, and a C-connector. The coil spring is inside the force generator. The choice of spring constant depends on the maximum feedback force. Moreover, if the spring constant is huge, the interface becomes more sensitive, and the noise will be increased. The L-connector connects with a load cell, and the C-connector connects with the input catheter. A rigid metal rod is used to simulate the input catheter. Using rigid rod instead of catheter can keep the natural manipulation skill of surgeon, and the rigid structure can transmit the force effectively.

The realization of haptic force feedback is shown in Fig. 3. When the operator manipulates the catheter, the motion x_s will change the length of the coil spring. The

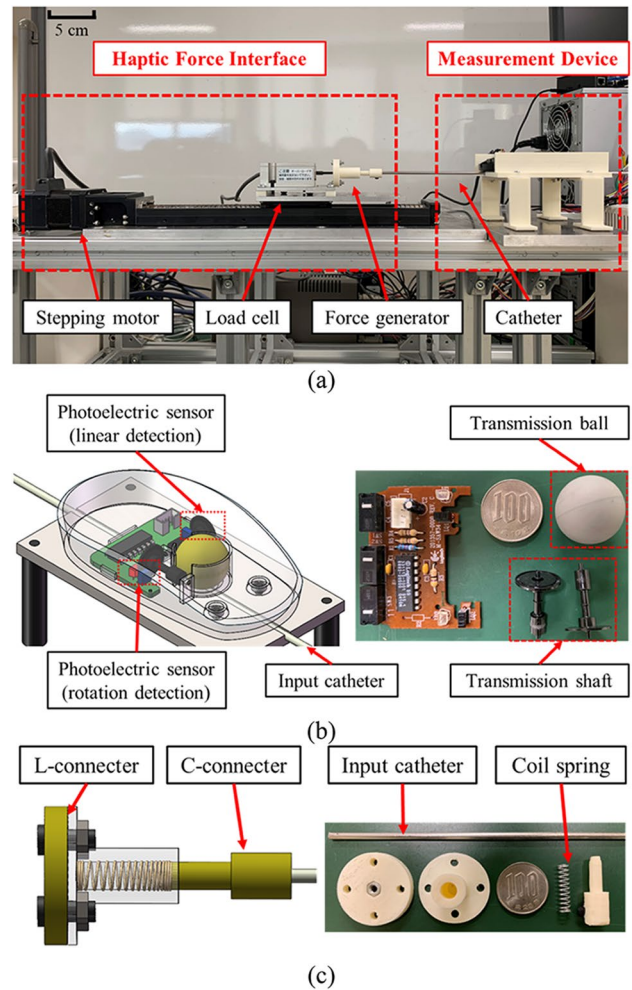


Fig. 2 The developed master side. a The master side. b Structure of measurement device. c Structure of force generator

deformation of spring will be converted into haptic force f_h , and it provides to the operator. The processing core compares haptic force f_h and proximal force f_s in real time and keep these two forces equal by using the motor

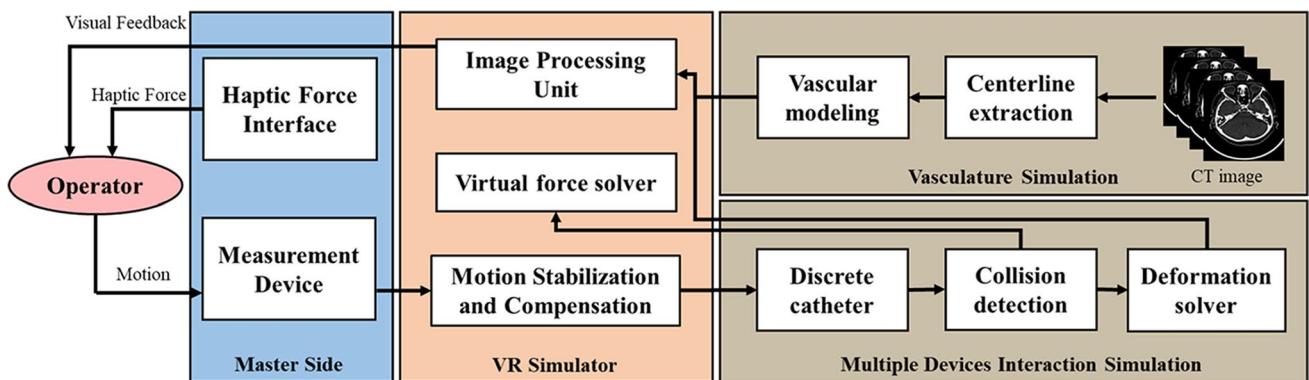


Fig. 1 An overview of our VR interventional training system

(VEXTA, ASM46AA, Oriental Motor Corp., Japan) to adjust the length of coil spring. It should be noticed that the human sensed feedback force is a resultant force, including the haptic force provided by haptic force interface and the friction force of measurement device. Owing to the haptic force adjusted by the motor, the operation speed for surgeon needs less than the max adjustment speed of haptic force interface. The haptic force interface is a closed loop system based on force signal. There has a load cell to measure the provided haptic force in real time, and the haptic force signal compares with the proximal force signal directly. Therefore, we can ensure the accuracy of provided haptic force.

The control of our system is achieved through two control boards. The motion signal of the measurement device is sent to the VR simulator through the motion control board (Arduino Mega2560, ELEGOO). The haptic control board (Arduino UNO, SMART Projects) processes the haptic force feedback. Control software is implemented using C++. The haptic control system and the motion control system are mutually independent, which can ensure non-interfering for each system.

2.2 VR simulator

The VR simulator is used to construct the virtual interventional environment. In the context of computer-based simulation of catheterization procedure, the virtual interventional environment can be established by patient-specific data. This makes the interventional training no longer limited to a few vasculature models, while reducing training costs. In order to realize interventional simulation, the simulator needs to contain two functions: reconstructing the vasculature mesh and simulating the behaviors of the surgical tools.

Vascular reconstruction is used to generate the vasculature mesh for the interventional training. The vasculature mesh includes classical vascular model (cardiovascular model, cerebrovascular model, etc.) and patient-specific vascular model. These vasculature models are reconstructed by iso-surfacing its segmented volume data. For vascular reconstruction, our group proposed a hybrid method for 3D vascular reconstruction. This method can reconstruct vascular model based on

computed tomography (CT) or magnetic resonance angiography images [22–26].

The simulation of the behaviors of the surgical tools is used to simulate the deformation and virtual contact force. This can make the simulation closer to the real surgeries. In the next section, we will introduce a novel method for simulating catheter interaction.

3 Catheter interaction simulating method

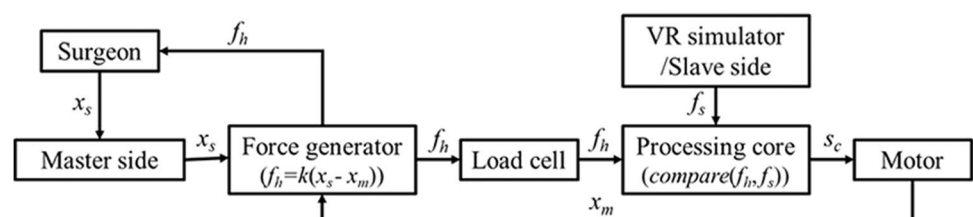
For VR interventional simulator, simulation of the behaviors of surgical tools (here mainly refers to catheter and guide-wire) is a challenging task. In this section, we introduce a novel numerical model to calculate the deformation and virtual contact force.

3.1 Simplified model of catheter behaviors

Human–machine interaction in virtual interventional simulation includes visual and haptic. In the context of MIS, the proximal force is the resultant force generated by the interaction between the surgical tools and the blood vessel [27]. For the VR interventional simulation, friction and collision were incorporated as the most influential forces applied to the instrument during the propagation within a vascular system [28]. The calculation of virtual contact force relies on the detection of the collision between virtual surgical tools and vasculature mesh, and simulation of the deformation of the virtual surgical tools is the key to obtain collision information.

In practice, the guidewire and the catheter are always coaxial in the course of the procedures. To avoid the complex interaction between the guidewire and the catheter, we use a single physical model (here is the catheter model) instead of catheter-guidewire combination. Moreover, because the propagation of twisting waves is much faster than bending waves in elastic rods, the catheters and guidewires can be treated as the material frame quasi-statically [29]. Therefore, we consider the catheter model as thin torsion-free elastic rod. It means that if we rotate the catheter, the whole catheter will rotate the same angle (rotate along the centerline of the catheter).

Fig. 3 Realization of haptic force feedback



3.2 Catheter modeling

In the procedures, the shape of the catheter is limited by the shape of the vasculature. The deformation of catheter depends on the applied force at the collision point, as shown in Fig. 4a. Our goal is to establish the relationship between the deformation and applied force.

We consider the catheter between two collision points as a thin torsion-free elastic rod. By solving for the shape of each elastic rod, we can obtain the whole shape of the catheter. For a uniform ideal elastic rod, it will be deformed when the end of the rod is applied an excessive force (the force active line is always located at the initial horizontal line, and the force-bearing points is always located at the end of the rod), as shown in Fig. 4b. The status of the rod with different applied force is:

$$\begin{cases} f \leq F_1, & \text{no deformation} \\ F_1 < f < F_2, & \text{deformation} \\ f = F_2, & \text{two force bearing points coincide} \end{cases} \quad (1)$$

where f is the applied force. F_1 and F_2 are the threshold of the applied force. If $f \leq F_1$, the elastic rod does not bend. If $f = F_2$, the ends of the bent elastic rod will coincide. If the cross-sectional area of the rod is neglected, the equilibrium state of the rod can be represented by the geometric shape S . Moreover, the deformation of the rod is affected by the applied force f . Therefore, we can get the relationship between the applied force f and bending moment M . Based on above analysis, the relationship between the deformation and applied force can be considered as the relationship between S and M .

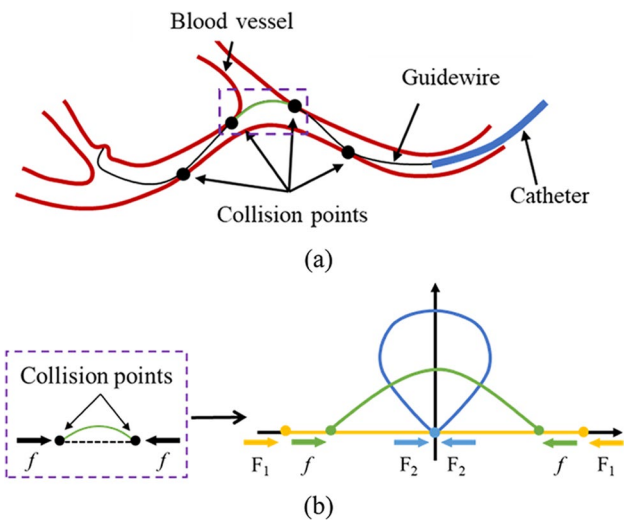


Fig. 4 Discretized catheter shape during the simulation. **a** Discretize the catheter by collision points. **b** The catheter between two collision points is treated as thin torsion-free elastic rods

3.2.1 Curvature of the geometric shape S

For a fixed-length elastic rod, if a force $f(f \in (F_1, F_2))$ is applied at the end, the deformation of the rod can be certain. Due to the geometry shape S of rod deformation is symmetrical, we can model a half of the shape first and then obtain the entire shape. To describe the geometry shape S of rod, we establish a 2D coordinate system, as shown in Fig. 5. The origin of the coordinate system is an end point of the rod. The direction of the applied force coincides with the Y -axis. The positive direction of the Y -axis is opposite to the applying force on the end point, and the positive direction of the X -axis is the same as the bending direction of the rod.

Supposing the angle between the tangent of an arbitrary point A in the curve and the positive direction of the X -axis is α , the angle increment between the positive direction of the X -axis and the tangent of point B , which the horizontal increment from point A is dx , is $d\alpha$. The differentiation of \widehat{AB} is ds . The curvature κ of point A is:

$$\kappa = \frac{d\alpha}{ds} \quad (2)$$

According to the theory of limit, when dx is close to 0, ds is close to D_{AB} (D_{AB} is the distance between the A and B). Thus, Eq. (2) can be expressed as:

$$\kappa = \frac{d\alpha}{D_{AB}} = \frac{d\alpha}{\frac{dx}{\cos\alpha}} = \frac{\cos\alpha d\alpha}{dx} \quad (3)$$

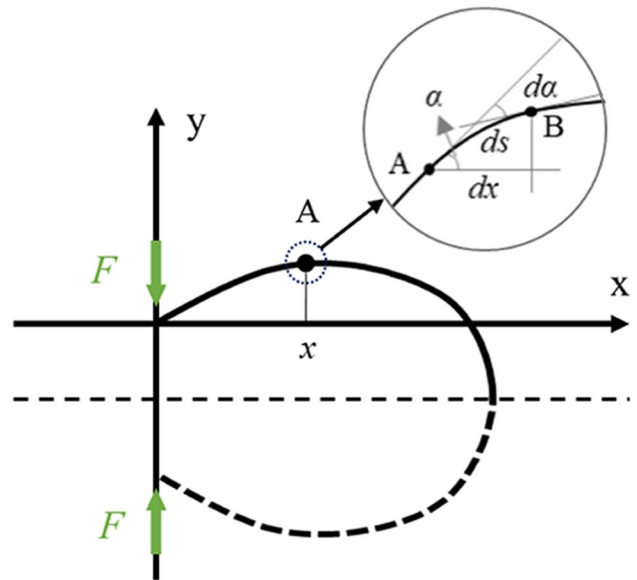


Fig. 5 Diagram of the curvature of a point on the elastic rod

3.2.2 Elasticity analysis for the thin torsion-free elastic rods

Given an ideal torsion-free elastic rod which the length is L , when we increase the applied a force f at the end of the rod, it will continue to deform. According to elementary beam theory, for an arbitrary point A in the rod during this period, we can obtain:

$$M = EI\kappa \tag{4}$$

where the κ , M , E , and I are the curvature of the point A, bending moment, elastic modulus of the rod, and moment of inertia, respectively. For an ideal catheter, the value of E and I is constant value. Let $p = 1/EI$, Eq. (4) can be transformed into:

$$\kappa = pM \tag{5}$$

In addition, the point A is balanced by the reaction force and the moment of the reaction force. The moment of force in the point A is:

$$M = fx \tag{6}$$

where the x is the coordinate of the point A on the X -axis (see Fig. 5).

3.2.3 Modeling

Considering that the half-shape is a convex curve (see Fig. 5), when $dx \geq 0$, the angle increment $d\alpha \leq 0$. According to Eqs. (3), (5), and (6), we can obtain:

$$pfx = -\frac{\cos \alpha d\alpha}{dx} \tag{7}$$

Let $k = pf$, Eq. (7) will be:

$$kxdx = -\cos \alpha d\alpha \tag{8}$$

We denote that at the end of the rod ($x = 0$), $\alpha = \alpha_0$. Based on the above conditions, the integral on both sides of the Eq. (8) can obtain:

$$\int_0^x kxdx = -\int_{\alpha_0}^{\alpha} \cos \alpha d\alpha \Rightarrow \frac{1}{2}kx^2 = \sin \alpha_0 - \sin \alpha \tag{9}$$

According to Fig. 5, we can obtain $\alpha \in [-\pi/2, \pi/2]$. Using the trigonometric formula, we can get:

$$\frac{dy}{dx} = \tan \alpha = \frac{\sin \alpha}{\sqrt{1 - \sin^2 \alpha}} \tag{10}$$

$$\frac{ds}{dx} = \frac{1}{\cos \alpha} = \frac{1}{\sqrt{1 - \sin^2 \alpha}} \tag{11}$$

Let $c = \sin \alpha_0$, which means that the sine of the angle between the tangent at the end point and the X -axis; according to Eqs. (9), (10), and (11), we can obtain the differential equation of the curve function of the equilibrium state of the rod:

$$dy = \frac{-\frac{1}{2}kx^2 + c}{\sqrt{1 - \left(-\frac{1}{2}kx^2 + c\right)^2}} dx \tag{12}$$

$$ds = \frac{1}{\sqrt{1 - \left(-\frac{1}{2}kx^2 + c\right)^2}} dx \tag{13}$$

3.2.4 Model solving

Based on above analysis, we get the differential equation of the curve function of the equilibrium state of the rod. However, this differential equation did not have a closed-form expression. Thus, we use numerical approximation to get the numerical solution. Because this model half of the shape, we can get $\int_0^{x_{max}} ds = L/2$, where L is the length of the rod and x_{max} is the maximum value of x . Due to $\alpha \in [-\pi/2, \pi/2]$, we can obtain the x_{max} by Eq. (9):

$$x_{max} = \sqrt{\frac{2(c + 1)}{k}} \tag{14}$$

Moreover, according to the range of α , we can obtain $c \in (-1, 1)$. The distance d_e between the two ends of the rod is $d_e = 2\left|\int_0^{x_{max}} dy\right|$. According to the above conditions, we can construct the numerical solution, as shown in Alg. 1.

3.3 Interaction simulation method

In order to simulate the behavior of catheter, our system should realize catheter shape simulation and virtual contact force calculation. The simulation process is shown in Fig. 6. During the simulation, the operator manipulates the catheter. When a collision between the catheter tip and vascular mesh is detected, the simulation method will calculate the deformation between two adjacent collision points and virtual contact force. Then, update the catheter shape, and provide virtual force feedback. The simulation method is summarized in Alg. 2.

3.3.1 Catheter shape

According to above analysis, we consider that the catheter is composed of a set of continuous elastic rods. For each elastic rod, the deformation is mainly affected by the force applied at the end points. By finding the deformation of each elastic rod, we can obtain the shape of the catheter. In SubSection 3.2,

we proposed a model to describe the relationship between the deformation and applied force for the elastic rod. To apply this model to simulate the catheter shape, we need to solve two problems: collision detection and deformation direction.

To achieve fast collision detection, we use a centerline-based distance detection method in our system, as shown in Fig. 7. Considering the difference of the radii of cross section for the vessel, the distance between the instrument and the centerline of the vessel is calculated as follows:

$$d_{err} = d_i - r_v \tag{15}$$

where d_i is the distance from the i -th joint of the catheter to the centerline and r_v is the radius of the vessel. If $d_{err} \geq 0$, a collision has been occurred. In the previous research, we proposed a centerline extraction method [30]. This method can extract the centerline and vessel radius from vasculature mesh. This method is applied in our VR interventional training system to help to realize collision detection.

The deformation direction of the catheter is affected by the normal vector of the contact plane of the end point, as shown in Fig. 8. If the direction of the normal vectors is the same (like p_1-p_2), the deformation direction is opposite to the normal direction. If the direction of the normal vectors is opposite (like p_2-p_3), the deformation is S-shaped.

3.3.2 Virtual contact force

In practice, the contact force is affected by many factors. It is difficult to use an accurate model to simulate the real contact force. In this research, we use a simple method to calculate the virtual contact force. This method is based on two characteristics of the contact force:

1. As the collision point increases, the contact force increases. The total force is the sum of the contact force for each collision point.
2. For a collision point, the contact force becomes larger as the angle between the normal line of the collision points and the direction of the catheter becomes smaller.

Based on the above conditions, the contact force for j -th collision point is calculated by:

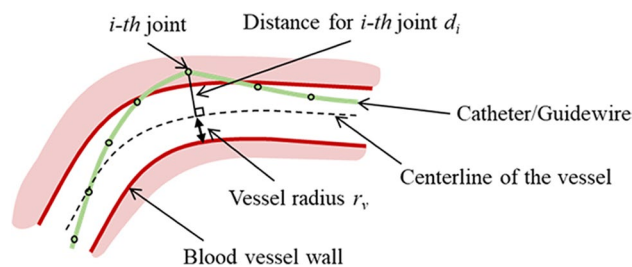


Fig. 7 2D illustration of collision detection method

$$f_j = \mu \cos \alpha_j \tag{16}$$

where μ and α_j are the force parameter and the angle between the normal line of j -th collision point and the direction of the catheter.

4 Experiment

In this section, two experiments have been done to evaluate the performance of the proposed method. Experiment 1 is used to verify the correctness of the model. Then, we apply the method to simulate the catheter interaction in VR interventional system, and the result is shown in Experiment 2.

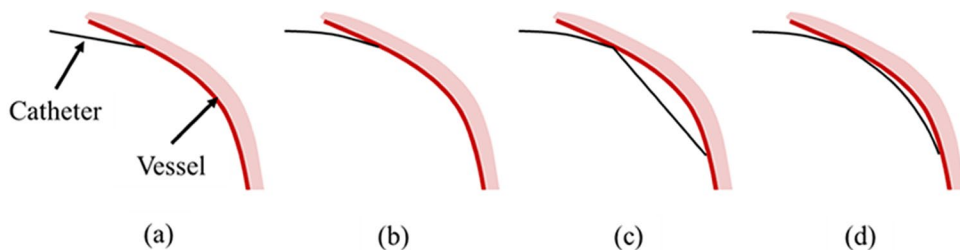
4.1 Model simulation

4.1.1 Experimental method

In Section 3.2, we proposed a method to simulate the deformation of elastic rod. In this experiment, we will verify the performance of the proposed model.

It should be noted that from a macro point of view, the “shape” is only determined by the parameter c ($c = \sin \alpha_0$, and α_0 is the angle between the tangent at the end point and the X -axis). The shape of a long elastic rod can be obtained by enlarging the shape of a short elastic rod. Therefore, we set the length of the elastic rod which is $L = 5$. Moreover, the step of parameter c and k is 0.001. The simulation software is MATLAB R2021a.

Fig. 6 2D illustration of simulation process. a The initial state at the beginning of simulation. b Calculate the catheter shape between two adjacent collision points. c Manipulate the catheter until next collision occurs. d Repeat the step in b



Input: the length of the rod l ; the deviation threshold v_t ; the maximum value of k ;

Output: Model parameter P ;

```

1: for  $c=-1$  to  $1$  do
2:   for  $k=0$  to  $k_{max}$  do
3:     # Determine the parameters  $c, k$  for length  $l$ 
4:     if  $\int_0^{x_{max}} \frac{1}{\sqrt{1-(\frac{1}{2}kx^2+c)^2}} dx - \frac{l}{2} < v_t$  then
5:       # Calculate the length of end of the rod
6:        $d_e = 2 * \left| \int_0^{x_{max}} \frac{-\frac{1}{2}kx^2+c}{\sqrt{1-(\frac{1}{2}kx^2+c)^2}} dx \right|$ ;
7:       # Calculate the shape  $(x, y)$ 
8:       for  $x=0, \dots, x_{max}$  do
9:          $y = \int_0^x \frac{-\frac{1}{2}kx^2+c}{\sqrt{1-(\frac{1}{2}kx^2+c)^2}} dx$ ;
10:        # Output the shape
11:         $C_s \leftarrow (x, y)$ ;
12:      end for
13:      # Save the parameter
14:       $P \leftarrow \{c, k, d_e, C_s\}$ ;
15:      # go to next step of  $c$ 
16:      break;
17:    end if
18:  end for
19: end for

```

Algorithm 1 S(l) - Catheter shape model

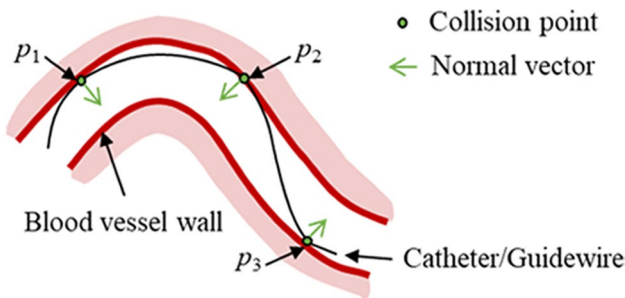


Fig. 8 2D illustration of the deformation direction of the catheter. For the catheter between p_1 and p_2 , the deformation direction is opposite to the normal direction. For the catheter between p_2 and p_3 , the catheter shape is S-shaped

4.1.2 Experimental result

To show the performance of the model, we chose 5 shapes with the applied force f_a to f_e , which satisfies the following conditions:

$$\begin{cases} f_a > f_b > f_c > f_d > f_e \\ f_a \approx F_1 \\ f_e \approx F_2 \end{cases} \quad (17)$$

Input: Catheter motion signal m_i ; model parameter P ;

Output: Catheter shape S_c ; virtual contact force F ;

```

1: initialization:
2: Initialize the vasculature mesh;
3: Set catheter initial position  $S_c \leftarrow m_0$ ;
4: Initialize the virtual contact force  $F = 0$ ;
5: Simulation loop:
6: while Start simulation do
7:   if  $m_i(i = 1, 2, \dots)$  is available then
8:     Detect the collision;
9:     if detect a collision  $p_j(j = 1, 2, \dots)$  then
10:      Calculate the distance  $l_j$  between  $p_j$  and
11:       $p_{j-1}$ ;
12:      for  $c_j=-1$  to  $1$  do
13:        # Extract parameters
14:         $(k, d_e, C_s) \leftarrow find(c_j == c)$ ;
15:        # Obtain catheter shape between  $p_j$ 
16:        and  $p_{j-1}$ 
17:         $C_j = C_s * (l_i/d_e)$ ;
18:        Detect collision between  $C_j$  and
19:        vasculature mesh;
20:        if Collision then
21:          break;
22:        end if
23:      end for
24:      # Update the catheter shape
25:       $S_c \leftarrow C_j$ ;
26:      Calculate the contact force  $f_j$ ;
27:       $F = F + f_j$ ;
28:    else
29:       $S_c \leftarrow m_i$ ;
30:    end if
31:  end while

```

Algorithm 2 Interventional simulation method

where the f_a approximates the critical value of the deformation (here we set $c = -0.999$, not -1) and f_e is approximately coincident at both end points. The result is shown in Fig. 9.

In addition, the shape of the elastic rod is determined by the parameter c . For a shape, the length of the elastic rod is related to the parameter k . Since k is proportional to f ($k = pf$, and p is a constant value), we can estimate the force by establishing the relationship between k and L . We calculate the value of k and L when $c = -0.999$, and the result is shown in Fig. 10. By using function to fit the result, we can obtain that the relationship between k and L is as follows:

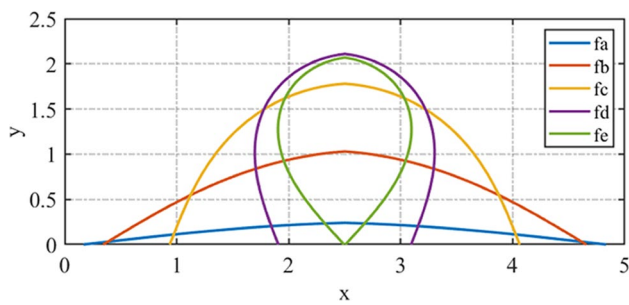


Fig. 9 Simulation result for the proposed numerical model

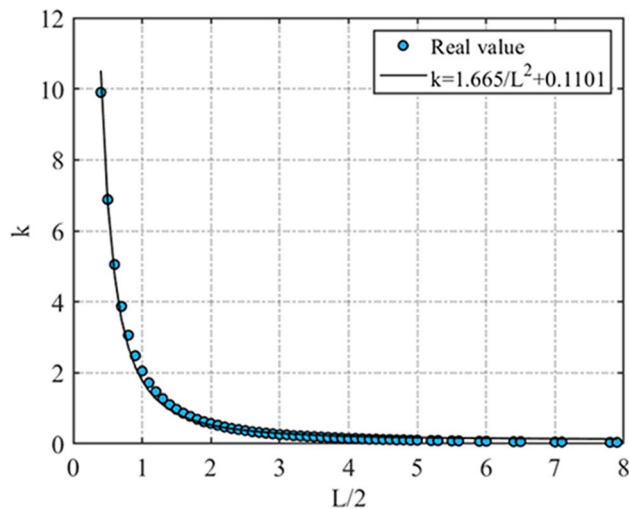


Fig. 10 The relationship of k-L

$$k = 1.665/L^2 + 0.1101 \tag{18}$$

Then, we can obtain:

$$f = (1.665/L^2 + 0.1101)/p \tag{19}$$

4.2 Performance in VR interventional training system

4.2.1 Experimental method

In this part, we will evaluate the performance of the proposed catheter interaction simulating method in the proposed VR interventional training system. The experiment includes two parts: catheter shape simulation and virtual contact force realization. The experimental setup is shown in Fig. 11. In VR simulator, we use a rigid vessel mesh. This rigid vessel mesh is established according to a rigid vessel model, and this makes it easier for us to

compare the difference between the simulation and the actual task. During the experiment, the operator manipulates the catheter through the master side. The operator does the same task, which is from point A to B, in the rigid vessel model and the rigid vessel mesh. The actual proximal force and the virtual contact force will be compared to illustrate the changing trend of the force during the experiment.

The VR simulation is conducted in a computer, which is equipped with an Intel Core i7-8750H CPU with 16 GB memory, and an NVIDIA GeForce GTX 1060 GPU. The operating system is Windows 10. We use OpenGL to do the rendering task, and the software is written in Python. The slave manipulator, which can measure the proximal force and manipulate the catheter, was proposed in previous research [31–37].

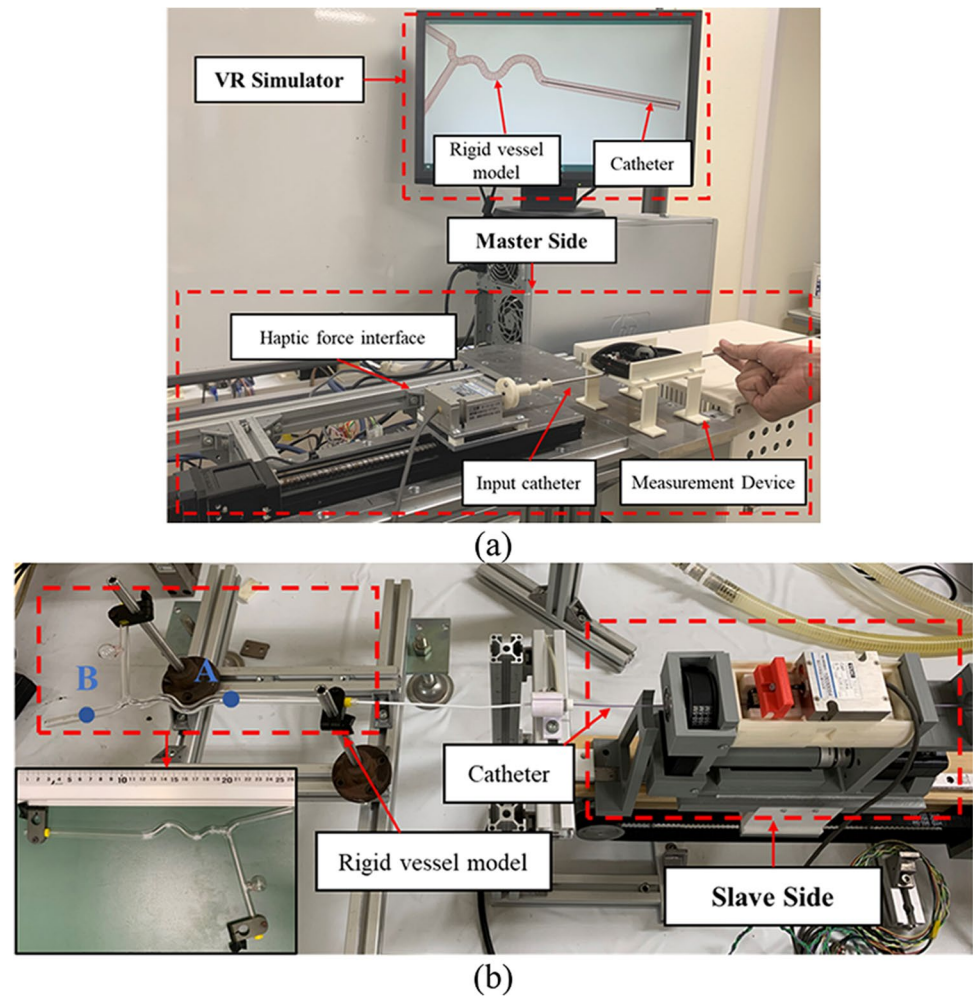
4.2.2 Experimental result

The simulation result is shown in Fig. 12. When the simulation starts, the catheter moves along the centerline of the vessel. When the virtual catheter tip contacts with vascular mesh, the catheter is deformed. The deformed catheter will replace the catheter which is between two adjacent collision points. When the collision point increases, the virtual contact force will increase. The virtual force comes from two aspects. One is the friction force between the catheter and blood vessel wall, and it is calculated by Eq. (16). Another is the deformation force of the catheter, and it is calculated by Eq. (19). During the simulation, the average running time for solving the deformation between two collision points is 12.27 ms. The processing time is much shorter than the human touch reaction time, and it satisfies the requirement of interventional simulation [38].

Meanwhile, we manipulate the catheter from target A to B by using slave manipulator, and the real contact force is recorded by a computer with a sampling frequency of 5 Hz. The real contact force and virtual contact force are compared in Fig. 13. The result shows that the changing trends of the virtual contact force and real contact force are the same. However, due to the complex interaction of catheter and blood vessel, the real force fluctuates. Compared with real force, the virtual force is steadily increasing.

Note that the purpose of this experiment is to evaluate the fidelity of our method by comparing the simulated behaviors of the catheter with that of a real one. The way the catheter is manipulated (will not happen in a real interventional procedure) intends to involve more collisions, aiming to show the accuracy of the proposed method within vascular models with high geometrical complexity. Thus, the shape of the catheter in this experiment may seem different from a real-life interventional procedure. However, it is shown in the

Fig. 11 Experimental setup for catheter interaction simulation. **a** The experimental platform is the proposed VR interventional training system. **b** Slave side is used for comparative evaluation



experiments that our method for simulating catheter interaction is enough to achieve satisfactory outcomes.

4.2.3 Discussion

Simulation of the behaviors of surgical tools is a challenging task for virtual interventional radiology. At present, there is still no perfect way to solve this problem. Current research, such as using FEM method or shared centerline method, is complicated, and it needs a lot of time to solve the model. Moreover, these methods did not consider the virtual contact force.

Our method can simulate the catheter shape and provide virtual contact force. However, it still cannot fully reproduce the behavior of the real catheter. One of the problems is that we simplified the model of catheter/guidewire, and it still not fully reproduced the physical properties of catheter/guidewire. Another problem is that in real-life interventional procedure, the collision point between the catheter and the blood vessel wall is not constant. Since blood vessels are smooth and dynamic, the collision point is not

fixed at a certain point. The movement of the collision point will change the shape of the catheter. In addition, due to the elasticity of the catheter and blood vessel wall, their contacts would be lines not only points. The future work is required to address these problems.

In the experiment, we use a rigid vessel model to establish the VR vessel model, not human vasculature. The human vascular system is a dynamic system with a beating heart. The future work will establish dynamic human vascular system, including heartbeat simulation and hemodynamics-based blood simulation and add these to our VR interventional system. In the future, we will improve our method to solve this problem.

5 Conclusion

In this paper, we develop a novel VR interventional training system. This system is an extension of the endovascular robotic system. Because the master side of this system can

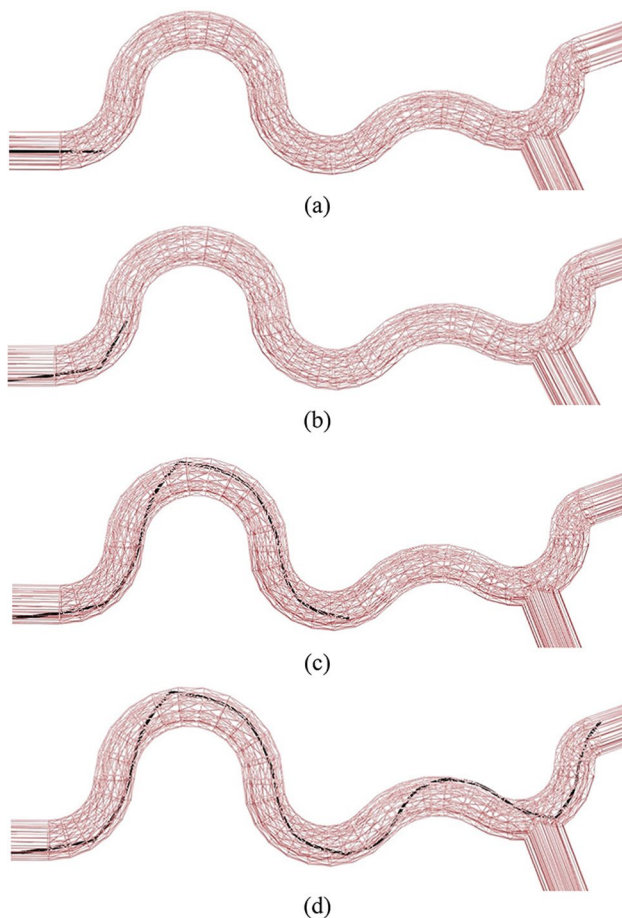


Fig. 12 Rigid vessel model intervention simulation. **a–d** Simulation result for different period of interventional task

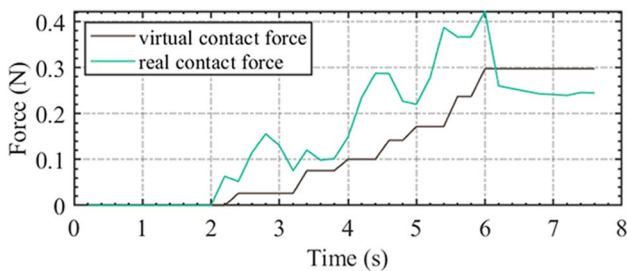


Fig. 13 Experimental result for comparison of proximal force and virtual force

also be used in the endovascular robotic system, the proposed system improves training and reduces the cost of education. In addition, a novel method is proposed to simulate the behaviors of surgical tools, including the deformation and virtual contact force. Our method discretizes the catheter by the collision points. For each part between two adjacent collision points, the catheter is treated as a thin

torsion-free elastic rod. Therefore, the catheter model is a structure composed of a set of elastic rods with different length. Based on this assumption, a novel numerical model is proposed to simulate the deformation of the catheter. Moreover, based on the characteristics of the contact force, we proposed an approximate method to simulate the virtual contact force. From the experimental studies, the proposed method for simulating catheter interaction is enough to achieve satisfactory outcomes. The average running time for solving the deformation between two collision points is 12.27 ms, which satisfies the requirement of interventional simulation. In the future, we will improve the performance of the catheter interaction simulation and apply the system in interventional training.

Acknowledgements This work was supported in part by the National High-Tech Research and Development Program (863 Program) of China under Grant 2015AA043202, and in part by SPS KAKENHI under Grant 15K2120.

References

- Shi P, Guo S, Zhang L, Jin X, Hirata H, Tamiya T, Kawanishi M (2021) Design and evaluation of a haptic robot-assisted catheter operating system with collision protection function. *IEEE Sens J* 21(18):20807–20816. <https://doi.org/10.1109/JSEN.2021.3095187>
- Guo S, Song Y, Yin X, Zhang L, Tamiya T, Hirata H, Ishihara H (2019) A novel robot-assisted endovascular catheterization system with haptic force feedback. *IEEE Trans Rob* 35(3):685–696. <https://doi.org/10.1109/TRO.2019.2896763>
- Yin X, Guo S, Xiao N, Tamiya T, Hirata H, Ishihara H (2016) Safety operation consciousness realization of a MR fluids-based novel haptic interface for teleoperated catheter minimally invasive neurosurgery. *IEEE/ASME Trans Mechatron* 21(2):1043–1054. <https://doi.org/10.1109/TMECH.2015.2489219>
- Bao X, Guo S, Xiao N, Li Y, Shi L (2018) Compensatory force measurement and multimodal force feedback for remote-controlled vascular interventional robot. *Biomed Microdevice* 20(3):74. <https://doi.org/10.1007/s10544-018-0318-0>
- Song Y, Guo S, Yin X, Zhang L, Hirata H, Ishihara H, Tamiya T (2018) Performance evaluation of a robot-assisted catheter operating system with haptic feedback. *Biomed Microdevice* 20(2):50. <https://doi.org/10.1007/s10544-018-0294-4>
- Zhao Y, Guo S, Wang Y, Cui J, Ma Y, Zeng Y, Liu X, Jiang Y, Li Y, Shi L, Xiao N (2019) A CNN-based prototype method of unstructured surgical state perception and navigation for an endovascular surgery robot. *Med Biol Eng Compu* 57(9):1875–1887. <https://doi.org/10.1007/s11517-019-02002-0>
- Yang C, Guo S, Bao X, Xiao N, Shi L, Li Y, Jiang Y (2019) A vascular interventional surgical robot based on surgeon's operating skills. *Med Biol Eng Compu* 57(9):1999–2010. <https://doi.org/10.1007/s11517-019-02016-8>
- Zheng L, Guo S (2021) A magnetorheological fluid-based tremor reduction method for robot-assisted catheter operating system. *Int J Mechatronics Automation* 8(2):72–79. <https://doi.org/10.1504/IJMA.2021.115234>
- Sankaran NK, Chembrammal P, Siddiqui A, Snyder K, Kesavadas T (2018) Design and development of surgeon augmented endovascular robotic system. *IEEE Trans Biomed Eng* 65(11):2483–2493. <https://doi.org/10.1109/TBME.2018.2800639>

10. Wang H, Wu J, Cai Y (2019) An adaptive deviation-feedback approach for simulating multiple devices interaction in virtual interventional radiology. *Comput Aided Des* 117:102738. <https://doi.org/10.1016/j.cad.2019.102738>
11. Wang Y, Serracino-Inglott F, Yi X, Yuan X-F, Yang X-J (2016) Real-time simulation of catheterization in endovascular surgeries. *Comput Animation Virtual Worlds* 27(3–4):185–194. <https://doi.org/10.1002/cav.1702>
12. Nowinski WL, Chui C-K (2001) Simulation of interventional neuroradiology procedures. *Proceed Int Workshop Med Imaging Augmented Reality*, 87–94. <https://doi.org/10.1109/MIAR.2001.930269>
13. Duriez C, Cotin S, Lenoir J, Neumann P (2006) New approaches to catheter navigation for interventional radiology simulation. *Comput Aided Surg* 11(6):300–308. <https://doi.org/10.3109/10929080601090623>
14. Li S, Guo J, Wang Q, Meng Q, Chui Y, Qin J, Heng P (2012) A catheterization-training simulator based on a fast multigrid solver. *IEEE Comput Graphics Appl* 32(6):56–70. <https://doi.org/10.1109/MCG.2012.32>
15. Li S, Qin J, Guo J, Chui Y-P, Heng P-A (2011) A novel FEM-based numerical solver for interactive catheter simulation in virtual catheterization. *Int J Biomed Imaging* 2011:815246. <https://doi.org/10.1155/2011/815246>
16. Alderliesten T, Bosman PAN, Niessen WJ (2007) Towards a real-time minimally-invasive vascular intervention simulation system. *IEEE Trans Med Imaging* 26(1):128–132. <https://doi.org/10.1109/TMI.2006.886814>
17. Alderliesten T, Konings MK, Niessen WJ (2007) Modeling friction, intrinsic curvature, and rotation of guide wires for simulation of minimally invasive vascular interventions. *IEEE Trans Biomed Eng* 54(1):29–38
18. Luboz V, Blazewski R, Gould D, Bello F (2009) Real-time guidewire simulation in complex vascular models. *Vis Comput* 25(9):827–834. <https://doi.org/10.1007/s00371-009-0312-x>
19. Luboz V, Zhang Y, Johnson S, Song Y, Kilkenny C, Hunt C, Woolnough H, Guediri S, Zhai J, Odetoynbo T, Littler P, Fisher A, Hughes C, Chalmers N, Kessel D, Clough PJ, Ward J, Phillips R, How T, ... Gould D (2013). *ImaGiNe Seldinger: First simulator for Seldinger technique and angiography training*. *Computer Methods and Programs in Biomedicine*, 111(2), 419–434. <https://doi.org/10.1016/j.cmpb.2013.05.014>
20. Alderliesten T, Konings MK, Niessen WJ (2004) Simulation of minimally invasive vascular interventions for training purposes. *Comput Aided Surg* 9(1–2):3–15. <https://doi.org/10.3109/10929080400006408>
21. Tran PT, Smoljkic G, Grijthuijsen C, Reynaerts D, Sloten JV, Poorten EV (2016) Position control of robotic catheters inside the vasculature based on a predictive minimum energy model. 2016 *IEEE Int Conference Syst, Man, Cybernetics (SMC)*, 4687–4693. <https://doi.org/10.1109/SMC.2016.7844971>
22. Guo J, Guo S (2017) Design and characteristics evaluation of a novel VR-based robot-assisted catheterization training system with force feedback for vascular interventional surgery. *Microsyst Technol* 23(8):3107–3116. <https://doi.org/10.1007/s00542-016-3086-x>
23. Gao B, Guo S, Xiao N, Guo J, Xiao X, Yang S, Qu M (2012) Construction of 3D vessel model of the VR robotic catheter system. *IEEE Int Conference Inform Automation* 2012:783–788. <https://doi.org/10.1109/ICInfA.2012.6246925>
24. Guo J, Guo S (2014) A haptic interface design for a VR-based unskilled doctor training system in vascular interventional surgery. *IEEE Int Conference Mechatronics Automation* 2014:1259–1263. <https://doi.org/10.1109/ICMA.2014.6885880>
25. Guo J, Guo S, Tamiya T, Hirata H, Ishihara H (2016) A virtual reality-based method of decreasing transmission time of visual feedback for a tele-operative robotic catheter operating system. *Int J Med Robot Comput Assisted Surg* 12(1):32–45. <https://doi.org/10.1002/rcs.1642>
26. Wang Y, Yang F, Li Y, Yang T, Ren C, Shi Z (2020) A tactile sensation assisted VR catheterization training system for operator's cognitive skills enhancement. *IEEE Access* 8:57180–57191. <https://doi.org/10.1109/ACCESS.2020.2982219>
27. Yin X, Guo S, Wang Y (2015) Force model-based haptic master console design for teleoperated minimally invasive surgery application. *IEEE Int Conference Mechatronics Automation (ICMA)* 2015:749–754. <https://doi.org/10.1109/ICMA.2015.7237579>
28. Aydin A, Raison N, Khan MS, Dasgupta P, Ahmed K (2016) Simulation-based training and assessment in urological surgery. *Nat Rev Urol* 13(9):503–519. <https://doi.org/10.1038/nrurol.2016.147>
29. Bergou M, Wardetzky M, Robinson S, Audoly B, Grinspun E. (2008). Discrete elastic rods. In *ACM SIGGRAPH 2008 papers* (pp. 1–12).
30. Shi P, Guo S, Jin X, Li X (2021) Centerline Extraction Method for virtual vascular model in virtual reality interventional training systems. *IEEE Int Conference Mechatronics Automation (ICMA)* 2021:1060–1064. <https://doi.org/10.1109/ICMA52036.2021.9512807>
31. Jin X, Guo S, Guo J, Shi P, Tamiya T, Hirata H (2021) Development of a tactile sensing robot-assisted system for vascular interventional surgery. *IEEE Sens J* 21(10):12284–12294. <https://doi.org/10.1109/JSEN.2021.3066424>
32. Jin X, Guo S, Guo J, Shi P, Tamiya T, Kawanishi M, Hirata H (2021) Total force analysis and safety enhancing for operating both guidewire and catheter in endovascular surgery. *IEEE Sens J* 21(20):22499–22509. <https://doi.org/10.1109/JSEN.2021.3107188>
33. Zhang L, Guo S, Yu H, Song Y (2017) Performance evaluation of a strain-gauge force sensor for a haptic robot-assisted catheter operating system. *Microsyst Technol* 23(10):5041–5050. <https://doi.org/10.1007/s00542-017-3380-2>
34. Zhang L, Guo S, Yu H, Song Y, Tamiya T, Hirata H, Ishihara H (2018) Design and performance evaluation of collision protection-based safety operation for a haptic robot-assisted catheter operating system. *Biomed Microdevice* 20(2):22. <https://doi.org/10.1007/s10544-018-0266-8>
35. Bao X, Guo S, Xiao N, Li Y, Yang C, Shen R, Cui J, Jiang Y, Liu X, Liu K (2018) Operation evaluation in-human of a novel remote-controlled vascular interventional robot. *Biomed Microdevice* 20(2):34. <https://doi.org/10.1007/s10544-018-0277-5>
36. Bao X, Guo S, Xiao N, Li Y, Yang C, Jiang Y (2018) A cooperation of catheters and guidewires-based novel remote-controlled vascular interventional robot. *Biomed Microdevice* 20(1):20. <https://doi.org/10.1007/s10544-018-0261-0>
37. Guo J, Jin X, Guo S, Fu Q (2019) A vascular interventional surgical robotic system based on force-visual feedback. *IEEE Sens J* 19(23):11081–11089
38. Kosinski RJ (2008) A literature review on reaction time. *Clemson Univ* 10(1):337–344

Publisher's note Springer Nature remains neutral with regard to jurisdictional claims in published maps and institutional affiliations.

Springer Nature or its licensor (e.g. a society or other partner) holds exclusive rights to this article under a publishing agreement with the author(s) or other rightsholder(s); author self-archiving of the accepted manuscript version of this article is solely governed by the terms of such publishing agreement and applicable law.



Peng Shi received the Ph.D. degree in Intelligent Mechanical Systems Engineering from Kagawa University, Takamatsu, Japan, in 2022. He is currently a lecturer with the School of Medical Technology and Engineering, Henan University of Science and Technology, Luoyang, China. He has published six refereed journal and conference papers. His research interests include catheter robotic systems, haptic feedback, and virtual reality systems.



Shuxiang Guo received the Ph.D. degree in Mechano-Informatics and Systems from Nagoya University, Japan, in 1995. He is currently the Chair Professor with the Key Laboratory of Convergence Medical Engineering System and Healthcare Technology, Ministry of Industry and Information Technology, Beijing Institute of Technology, Beijing, China. He has published about 710 refereed journals and conference papers. His research interests include micro-catheter systems, medical robot systems for

minimal invasive surgery, biomimetic underwater robots, and smart material (SMA and IPMC) based on actuators. Prof. Guo is an Editor-in-Chief for the International Journal of Mechatronics and Automation.



Xiaoliang Jin received the Ph.D. degree in Intelligent Mechanical Systems Engineering from Kagawa University, Takamatsu, Japan, in 2022. He is currently a post-doc in the State Key Laboratory of Bioelectronics and the Jiangsu Key Laboratory of Remote Measurement and Control, School of Instrument Science and Engineering, Southeast University, Nanjing, China. He has published eight refereed journal and conference papers. His research interests include catheter robotic systems, force control, and haptic feedback.



Hideyuki Hirata received the B.S. and M.S. degrees in Mechanical Engineering from Yokohama National University, Yokohama, Japan, in 1981 and 1983, respectively, the Ph.D. degree in Mechanical Engineering from Tokyo Institute of Technology, Tokyo, Japan, in 1992. He is currently Professor with the Faculty of Engineering and Design, Kagawa University, Takamatsu Japan. He has published about 40 refereed journal and conference papers.

His current research includes material strength, material design, and microdevices based on computer simulation technology.



Takashi Tamiya received the Ph.D. degree in Neuro logical Surgery from the Medical School of Okayama University, Okayama, Japan, in 1990. He had fellowships with Massachusetts General Hospital, Harvard Medical School in the USA from 1993 to 1994. He is currently a Full Professor with the Faculty of Medicine, Kagawa University, Takamatsu, Japan. He has published over 400 refereed journal and conference papers. His current research includes the surgical techniques of neurosurgical operations and intravascular surgery system.



Masahiko Kawanishi received the B.S. degree from the Faculty of Medicine of Kagawa Medical University, Kagawa, Japan, in 1993. He is currently a lecturer with the Faculty of Medicine, Kagawa University, Takamatsu, Japan. He has published over 80 refereed journal and conference papers. His current research includes the surgical techniques of neurosurgical operations and intravascular surgery system.